Supplementary Material

Human breast, lung, colon, and pancreatic tissue specimens, DNA extraction

An archival collection of formalin-fixed, paraffin-embedded, human breast (n = 25), lung (n = 30), colon (n = 30), and pancreatic (n = 30) tumors were subjected to DNA extraction by using the QuickExtract™ FFPE DNA Extraction Kit (Epicentre Biotechnologies, Madison, WI) following the manufacturer's manual. Institutional Review Board approval was obtained at participating hospitals and the National Institutes of Health.

Real-time RT–PCR

Primers for *Ha-Ras*, *Ki-Ras*, *N-Ras*, *RASA1-4*, *nGAP*, *SYNGAP1*, *hDAB2IP*, *RASAL1*, *NF1*, *PITX1*, and ribonucleic acid ribosomal 18S (*RNR-18*, internal control) genes were from Applied Biosystems (Foster City, CA). PCR reactions were performed with 100 ng of cDNA, using an ABI Prism 7000 Sequence Detection System and TaqMan Universal PCR Master Mix (Applied Biosystems). Cycling conditions were: 10 min of denaturation at 95°C and 40 cycles at 95°C for 15 s and at 60°C for 1 min. Quantitative values were calculated by using the PE Biosystems Analysis software and expressed as N target (NT). $NT = 2^{-\Delta Ct}$, wherein ΔCt value of each sample was calculated by subtracting the average Ct value of the target gene from the average Ct value of the *RNR-18* gene.

Western blotting, immunoprecipitation

Six normal livers, 30 HCCB, 30 HCCP, and respective non-neoplastic surrounding livers were homogenized in lysis buffer [30 mM Tris (pH 7.5), 150 mM NaCl, 1% NP-40, 0.5% Na deoxycholate, 0.1% SDS, 10% glycerol, and 2 mM EDTA] containing the Complete Protease Inhibitor Cocktail (Roche Molecular Biochemicals, Indianapolis, IN) and sonicated. Protein concentrations were determined with the Bio-Rad Protein Assay Kit (Bio-Rad, Hercules, CA) using bovine serum albumin as standard. For western blotting, aliquots of 40 μg were

denatured by boiling in Tris-Glycine SDS Sample Buffer (Invitrogen, Carlsbad, CA), separated by SDS-PAGE, and transferred onto nitrocellulose membranes (Invitrogen) by electroblotting. Membranes were blocked in 5% non-fat dry milk in Tris-buffered saline containing 0.1% Tween 20 for 1 h and probed with specific antibodies listed in Supplementary Table 2. Each primary antibody was followed by incubation with horseradish peroxidase-secondary antibody diluted 1:5000 for 1 h and then revealed with the Super Signal West Pico (Pierce Chemical Co., New York, NY). For each protein, densities were calculated by ImageQuaNT 5.1 software (GE Healthcare, Piscataway, NJ), normalized to β-actin (Chemicon International, Temecula, CA; dilution 1:20000) levels and mean values evaluated for statistical significance. For immunoprecipitation studies, a total of 500 μg of liver tissue lysates were immunoprecipitated with 5 μg of agarose conjugated antibodies. As negative controls, antibodies used for immunoprecipitation were neutralized, prior to IP, by a preincubation of 2 h at room temperature with the respective immunogen peptide (I :20 w/w), which resulted in inhibition of the immunoprecipitation.

Ras activation assay

Levels of activated Pan-, Ha-, Ki-, and N-*R*as (Pan-, Ha-, Ki-, and N-*R*as-GTP) bound to RAF-1 were determined in 6 normal livers, 30 HCCB and 30 HCCP, and corresponding non-neoplastic liver tissues by using the *R*as Activation Assay Kit (Millipore, Billerica, MA) following the manufacturer's instructions. Briefly, liver tissues were homogenized in a lysis buffer containing 125 mM HEPES, pH 7.5, 750 mM NaCl, 5% Igepal CA-630, 50 mM MgCl2, 5 mM EDTA, 10% glycerol and proteinases inhibitors. Aliquots of 500 μg of liver tissue lysate were subjected to Ras pull-down assay by overnight incubation with 10 μg of Raf-1 RBD agarose. Proteins were separated via SDS-PAGE, transferred onto nitrocellulose membranes and probed with antibodies anti-Pan-, Ha-, Ki-, and N-Ras (Santa Cruz Biotechnology, Santa Cruz, CA) followed by incubation with the secondary antibody.

Assessment of Ras GEF activity

Ras-agarose (0.25 μg) was incubated in 50 μL of reaction buffer [25 mmol/L Tris-HCl (pH 7.5), 5 mmol/L MgCl2, 1 mmol/L DTT, and 100 μg of bovine serum albumin] with 100 μmol/L unlabeled GDP at 37ºC for 30 min. Tissue lysates (10 μg) were added to the unlabeled GDP *Ras*-agarose complex in the presence of 10 μCi of [3H]GDP (GE Healthcare) and 18 mmol/L MgCl2 at 37ºC for 10 min. The *Ras*-agarose complex was pulled down, washed three times with the reaction buffer, and the amount of bound *Ras*-[^{3}H]GDP was determined by a Beckman Coulter (Fullerton, CA) scintillation counter. Addition of 2 mmol/L GTP-γ-S to the mix of [^{3}H]GDP, tissue lysates, and unlabeled GDP *Ras*-agarose complex, abolished the exchange reaction.

Methylation-specific PCR, combined bisulphite restriction analysis (COBRA), and microsatellite analysis

Genomic DNA from 10 normal livers, 88 HCCs (41 HCCB and 47 HCCP) and matching non-tumorous surrounding livers as well as genomic DNA from a collection of human breast (n = 25), lung (n = 30), colon (n = 30), and pancreatic (n = 30) tumors was modified by using the EZ DNA methylation kit (Zymo Research, Orange, CA). The CpGenome Universal Methylated DNA and CpG Universal Unmethylated DNA (Millipore, Billerica, MA) were used as positive and negative control for each reaction, respectively. Primers to assess the promoter status of *PITX1* were designed using the MethPrimer software, and those for *RASAL1*, *DAB2IP*, and *NF1* genes were previously generated. A total of 30 ng of DNA was amplified in a reaction volume of 15 μl consisting of 0.4 μM each primer, 200 μM each dNTP, 10x PCR buffer, 5x GC-RICH solution, and 0.4 U of FastStart Taq DNA Polymerase (Roche Molecular Biochemicals, Indianapolis, IN). Presence of promoter hypermethylation was defined as the amplification of the specific PCR product of the investigated gene when using methylated-specific primers. Promoter hypermethylation was further confirmed by using the

combined bisulphite restriction analysis (COBRA) method. COBRA was performed as previously described (Supplementary Reference 1). In brief, primers used in the PCR reaction did not contain CpG dinucleotides so that the amplification step does not discriminate between templates according to their original methylation status. PCR products were then digested with the 100 units of the restriction enzyme BstUI (New England Biolabs, Ipswich, MA), which cleaves only methylated sites containing the CGCG recognition sequence. Next, diagnostic fragments were resolved on a 10% polyacrylamide gels, stained with SYBR® Green I nucleic acid gel stain (Invitrogen, Carlsbad, CA), and photoimaged with a UV camera. Loss of heterozygosity (LOH) of *RASAL1*, *hDAB2IP*, *NF1*, and PITX1 gene loci was investigated with D12S78, D12S79, D9S258, D9S1821, D17S1788, D17S2103, D5S2056, and D5S2115 primer pairs, as published (26). LOH was recorded when a 50% or greater reduction in electrophoretic band intensity was detected with SYBR® Green I nucleic acid gel stain (Invitrogen). Sequence and product size of primers used for methylation-specific PCR, COBRA, and microsatellite analyses are shown in Supplementary Table 3.

Microvessel density (MVD) evaluation

To assess HCC intratumoral vascularity, microvessel density (MVD) was evaluated as reported (Supplementary Reference 2). Briefly, HCCs were stained with a mouse monoclonal antibody against the endothelial cell marker CD34 (Vector Laboratories, Burlingame, CA). Any brown-stained endothelial cell or endothelial cell cluster was counted as one microvessel, irrespective of the presence of a vessel lumen. Tumors were first screened at low power (x 40) to identify the areas of highest MVD. The four highest MVD areas for each tumor were photographed at high power (x 200) and the size of each area standardized using the ImageJ 1.41 software. MVD was expressed as the percentage (mean ± SD) of the total CD-34-stained spots per section area (0.94 mm^2). Pearson's correlation testing was used to assess the correlation between DAB2IP levels and MVD by PRISM 2.00 (GraphPad Software).

Cell Lines, treatments, viability, apoptosis, and vascular endothelial growth factor-α secretion assays

Human HCC cell lines (HuH6, Hep3B, SNU449, PLC/Alexander, Focus, and SNU389) were maintained as monolayer cultures in Dulbecco's modified Eagle medium supplemented with 10% fetal bovine serum. 2.0 x 10^3cells were plated per well in 96-well plate and grown for 12 h. For silencing experiments, HCC cell lines were then serum deprived for 24 h and treated with small interfering RNA (siRNA) against RASAL1, DAB2IP, and PITX1 as described Supplementary References 3,4,5). Transient transfection experiments with wild-type or dominant-negative mutant (S17N) *Ha-Ras*, and *ERK2* (wild-type) cDNA in pUSEamp plasmid (Millipore), wild-type *RASAL1*, *DAB2IP*, or *PITX1* cDNAs in pCMV6-XL5 plasmid (OriGene Technologies, Rockville, MD) were conducted following the manufacturer's protocols. Cell viability, apoptosis, and vascular endothelial growth factor-α (VEGF-α) secretion were determined by WST-1 Cell Proliferation Reagent, Cell Death Detection Elisa Plus kit (Roche Molecular Biochemicals, Indianapolis, IN), and VEGF-α ELISA kit (R&D Systems, Minneapolis, MN), respectively, according to the manufacturers' instructions. Apoptosis was assessed both in basal condition and following treatment with l μM Staurosporine for 4 h. For Zebularine treatment, Focus and SNU389 cell lines were plated at a density of 2.0 × 10^6 cells in 10-cm dishes and treated with Zebularine (200 μmol/L) for 24–72 hours.

Supplementary References

1. Z. Xiong,. P.W. Laird. COBRA: a sensitive and quantitative DNA methylation assay. *Nucleic Acids Res* **25** (1997), pp. 2532-2534.
2. N. Tanigawa, N. Lu, C. Mitsui, S. Miura. Quantitation of sinusoid-like vessels in hepatocellular carcinoma: its clinical and prognostic significance. *Hepatology* **26** (1997), pp. 1216-1223.
3. H. Jin, X. Wang, J. Ying, A.H. Wong, Y. Cui, G. Srivastava, *et al*. Epigenetic silencing of a Ca(2+)-regulated Ras GTPase-activating protein RASAL defines a new mechanism of Ras activation in human cancers. *Proc Natl Acad Sci U S A* **104** (2007), pp. 12353-12358.
4. W. Min, Y. Lin, S. Tang, L. Yu, H. Zhang, T. Wan, *et al*. AIP1 recruits phosphatase PP2A to ASK1 in tumor necrosis factor-induced ASK1-JNK activation, *Circ Res* **102** (2008), pp. 840-848.
5. D.X. Liu, P.E. Lobie. Transcriptional activation of p53 by Pitx1. *Cell Death Differ* **14** (2007), pp. 1893-1907.

Supplementary Table 1. Clinicopathological features of HCC Patients

Variables	Features	
	HCCB[a]	HCCP[b]
No. of patients	41	47
Male	35	40
Female	6	7
Age (Mean ± SD)	58.4 ± 14.10	57.5 ± 15.42
Etiology		
HBV	18	21
HCV	14	16
Ethanol	8	7
Wilson disease	0	1
Hemochromatosis	1	2
Cirrhosis		
+	28	36
-	13	11
Tumor size		
> 5 cm	25	31
< 5 cm	16	16
Edmondson and Steiner grade		
I	5	3
II	12	10
III	10	14
IV	4	20
Alpha-fetoprotein secretion		
> 300 ng/ml of serum	14	17
< 300 ng/ml of serum	27	30
Survival after partial liver resection (months) Means ± SD[f]	98.24 ± 36.55	18.44 ± 9.20

[a]HCCB, HCC with better prognosis

[b]HCCP, HCC with poorer prognosis

Supplementary Table 2. List of the primary antibodies used for western blotting and immunoprecipitation analysis

Protein	**Antibody**	**Epitope mapping**
Pan-*Ras*	Mouse monoclonal	Full length†
Ha-*Ras*	Mouse monoclonal	Full length†
Ki-*Ras*	Mouse monoclonal	Amino acids 54-189†
N-*Ras*	Mouse monoclonal	Full length†
RASAL1	Goat polyclonal	COOH terminus#
NF1	Rabbit polyclonal	COOH terminus#
PITX1	Mouse monoclonal	Full length†
pRAF-1	Rabbit monoclonal	pSer338*
ERK2	Mouse monoclonal	COOH terminus†
c-JUN	Mouse monoclonal	Amino acids 1-79†
c-Fos	Rabbit polyclonal	NH_2 terminus†
ASK1	Goat polyclonal	NH_2 terminus†
pASK1	Rabbit polyclonal	pSer83*
pP38 MAPK	Mouse monoclonal	pTyr182†
pJNK	Mouse monoclonal	pThr183/Tyr185†
14-3-3 β	Rabbit polyclonal	NH_2 terminus†
VEGFR2 (FLK-1)	Mouse monoclonal	COOH terminus†
pPLC-γ	Rabbit polyclonal	pTyr783*
pAKT	Rabbit polyclonal	pSer473*
P85	Rabbit polyclonal	COOH terminus*
ACTIN	Rabbit polyclonal	COOH terminus†

† Provided by Santa Cruz Biotechnology (Santa Cruz, CA).
#Provided by Novus Biologicals (Littleton, CO).
* Provided by Cell Signaling Technology Inc. (Danvers, MA).

Supplementary Table 3. Sequence and product size of unmethylated (U)- and methylated (M)-specific primers for RASAL1, DAB2IP1, NF1, and PITX1 promoters used in methylation-specific PCR, for combined restriction bisulphite analysis (COBRA) of RASAL1, DAB2IP, NF1, and PITX1 promoters, and for RASAL1, DAB2IP1, NF1, and PITX1 loci used in microsatellite analysis

Primer name	Sequence		Product size (bp)
	Forward	Reverse	
RASAL1-U	AATTTATTAGGAGTTAGTGGTTAT	CACAACAAACTCTTACCAAAACA	140
RASAL1-M	GTGTATTTTTGTTTTCGTCGTTC	CAACGAACTCTTACCGAAACG	152
RASAL1 COBRA	GTTTAATGTTAATTTATTAGGAGTT	CTAACCACAAACTTTCCAAACAA	315
DAB2IP-U	GAGGTGAGTGGGGTGGTT	CACTATTACCTTAACAACACCAA	163
DAB2IP-M	GAGGTGAGCGGGGCGGTC	CGCTATTACCTTAACGACGCCGA	163
DAB2IP COBRA 1	GGATTTTTTTAGGTGGGTGT	CCCTAAACCRCTATTACCTTAAC	236
DAB2IP COBRA 2	GTTAAGGTAATAGYGGTTTAGGG	ACRAACTCACCTCTCATTATCC	397
NF1-U	TGTTTGTTAGATGGTTTAGAGGAGTTAGATGAT	AAAAACAAAAAAAAAAAACAACCTACCACA	125
NF1-M	CGTTAGACGGTTTAGAGGAGTTAGATGAC	AAAAAAAAAACGACCTACCGCG	120
NF1 COBRA 1	AGTTTAAGTTGAGAGTATAGTTTTTTTAGG	TCTCCCCACAACCATCACAATCC	489
NF1 COBRA 2	GATTGTGATGGTTGTGGGGAG	CAAAACCTAAAACAACC(AG)CAAAAAAAAC	468
PITX1-U	TTGGAGTTTTAGAAATTGGTTTTG	ACAACTTCTCACAACTAAACACC	135
PITX1-M	CGGAGTTTTAGAAATCGGTTTC	AACTTCTCGCGACTAAACGC	132
PITX1 COBRA	ATTGTTGGAATTTGGTTGTG	AACCCCATATCATAAAATAAC	467
D12S78	CTTTGCAGCACCATGTATTT	ACTGCTGGCTTTAACAGAAA	171/201
D12S79	GTTGGACTGAACTGAGATGC	GCACCCAGACTACCATATAATC	155
D9S258	TAGAGATGCCCTTGAGTGAA	ATCAATTTGGATCCTTCAGG	170
D9S1821	AACTGTGATGGATACACGAAC	CACCAGGAAACTGACTTGATAC	168/174
D17S1788	TGCAGATGCCTAAGAACTTTTCAG	GCCATGATCTCCCAAAGCC	156/168
D17S2103	GGATCAAGGAATCACTTGAAGTTAG	CAGTAACGGATGGTATCATTGGAG	182
D5S2056	GAGCCTGAGANGTCAAGACT	AAGCCTCCCACCTCTG	162/206
D5S2115	GGCACTCATGCTGCACT	GTAAGCCCCTGGCTCCT	251/277

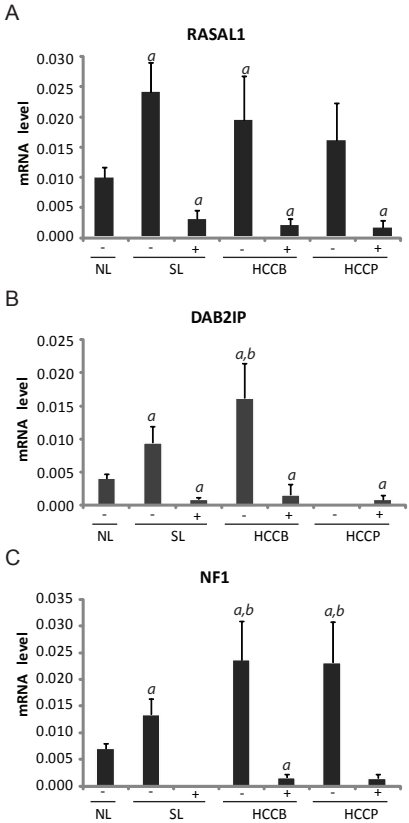

Supplementary Figure 1. Effect of promoter methylation on mRNA expression levels of RASAL1 (A), DAB2IP (B), and NF1 (C) RAS GAPs in human HCC. Promoter methylation was determined by methylation-specific PCR and combined bisulphite restriction analysis (COBRA) assay. Levels of expression of RASAL1, DAB2IP, and NF1 genes by quantitative reverse-transcription real-time PCR in normal livers (NL), surrounding non-tumorous livers (SL), and HCC characterized by better (HCCB) or poor prognosis (HCCP). N Target (NT) = $2^{-\Delta Ct}$, where ΔCt value of each sample was calculated by subtracting the Ct value of the target gene from Ct value of the RNR-18 gene. Data are means ± SD. Multiple comparison test (Kruskal-Wallis) $p < 0.05$ *a*, *vs* N.L.; *b*, *vs* SL; *c*, *vs*. HCCB. -, unmethylated; +, methylated.

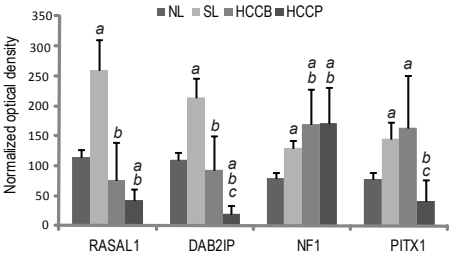

Supplementary Figure 2. RASAL1, DAB21P, NF1 and PITX1 protein levels in human liver (NL), HCC with better or poor prognosis (HCCB and HCCP,respectively) and in the corresponding surrounding livers (SLB and SLP). Data are the means ± SD of 10 normal livers, and 41 HCCB and SLB, and 47 HCCP and SLP. Abbreviations HCCB and HCCB, HCC with better and poor prognosis, SLB and SLP, surrounding livers with better and poor prognosis. Multiple comparison test (Kruskal-Wallis) $p < 0.05$ a, vs. NL; b vs. SL; c vs. HCCB.

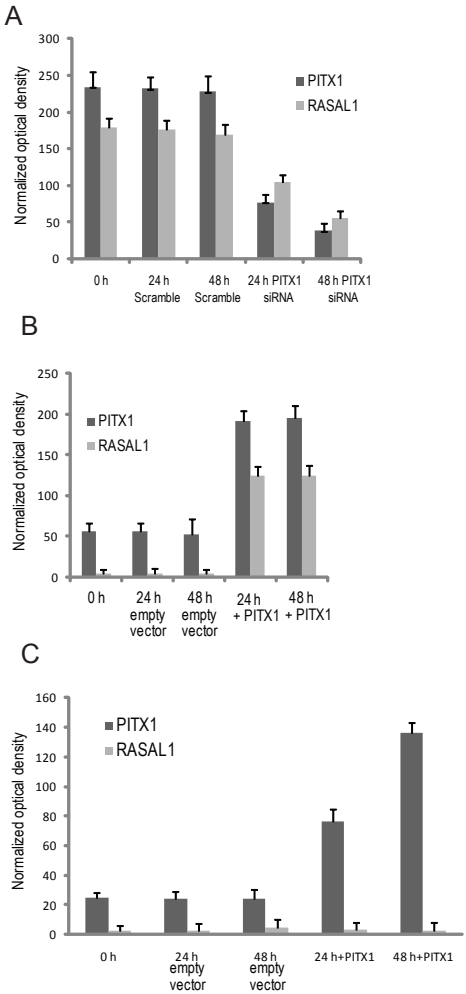

Supplementary Figure 3. Densitometric analysis of the effect of the manipulation of PITX1 expression on RASAL1 levels. (A) siRNA of PITX1 in HUH6 cells. (B,C) PITX1 cDNA transfectionin SNU449 cells (B) and PLC/Alexander (C) cells, harboring a RASAL1 unmethylated and methylated promoter, respectively. Protein lysates were subjected to western blot analysis with specific antibodies for each protein, densities were calculated by ImageQuaNT 5.1 software (GE Healthcare, Piscataway, NJ) and normalized to β-Actin (Chemicon International,Temecula, CA; 1:20000) levels. Statistical significance (A) Student *t* test, $p < 2.38 \times 10^{-3}$ and (B, C) Mann-Whitney test, $p < 3.56 \times 10^{-3}$.

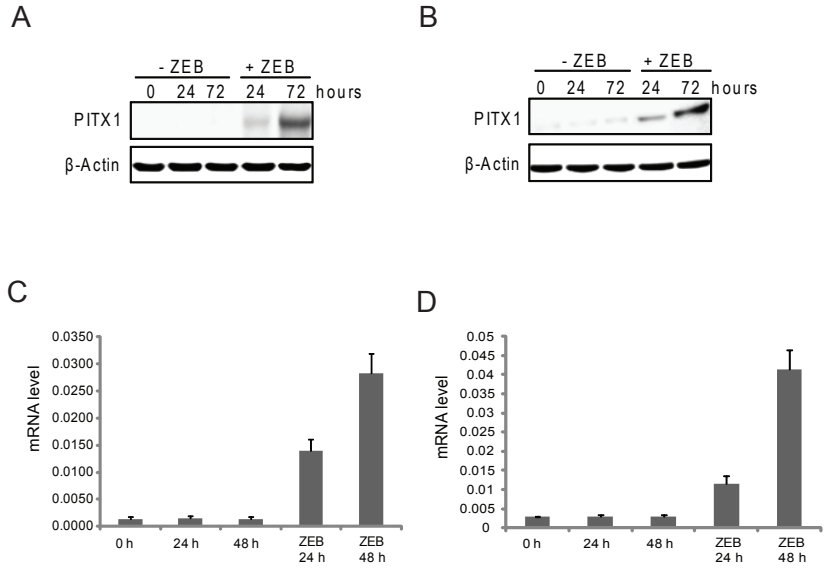

Supplementary Figure 4. Reactivation of PITX1 gene following treatment with the hypomethylating agent Zebularine (ZEB). Focus (A,C) and SNU389 (B,D) human HCC cell lines were used. PITX1 levels were assessed both via western blot (A,B) and real-time reverse-transcription PCR (C,D) analysis. Focus and SNU389 cells were plated at a density of 2.0 x 10^6 cells in 10-cm dishes and treated with Zebularine (200 μmole/L) for 24-72 hours

A

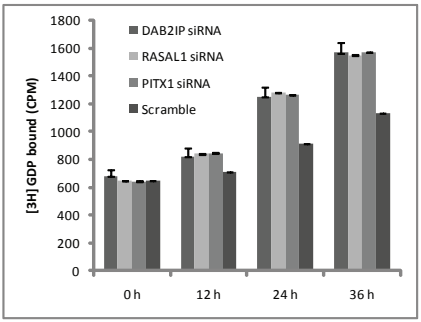

B

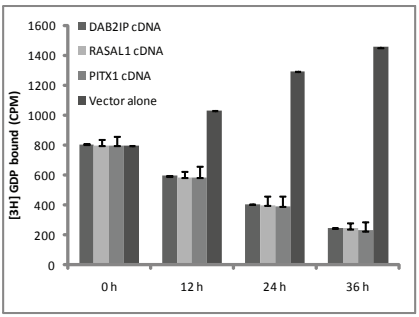

Supplementary Figure 5. Effect of manipulating RASAL1, DAB2IP, and PITX1 expression on Ras GEF activity in human HCC cell lines. (A) Silencing of RASAL1, DAB2IP or PITX1 via siRNA increased Ras GEF activity in HuH6 cells. Equivalent results were obtained in Hep3B cells (not shown). (B) Overexpression of RASAL1, DAB2IP or PITX1 by transient transfection reduces Ras GEF activity in SNU449 cells. To assess Ras GEF activity, Ras-agarose (0.25 µg) was incubated in 50 µL of reaction buffer [25 mmol/L Tris-HCl (pH 7.5), 5 mmol/L MgCl2, 1 mmol/L DTT, and 100 µg of bovine serum albumin] with 100 µmol/L unlabeled GDP at 37ºC for 30 min. HCC cell lysates (10 µg) were added to the unlabeled GDP Ras-agarose complex in the presence of 10 µCi of [3H]GDP and 18 mmol/L MgCl2 at 37ºC for 10 min. Ras-agarose complex was pulled down, washed three times with the reaction buffer, and the amount of bound Ras-[3H]GDP was determined by a Beckman Coulter scintillation counter. Experiments were repeated at least 3 times in triplicate. Each bar represents mean ±SD. One way ANOVA(A) or Kruskal-Wallis(B), treated vs control (scramble or vector alone) $p < 0.05$ at all time points.

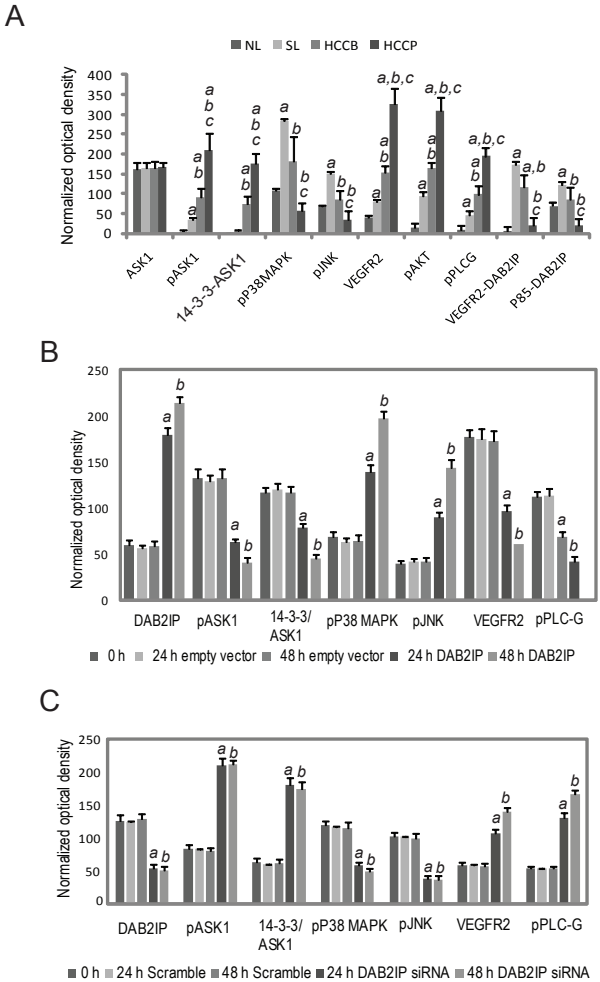

Supplementary Figure 6. Densitometric analysis of the levels of DAB2IP interactors (A)and the effect of the manipulation of DAB2IP expression on the levels of the ASK1/P38MAPK/JNK and VEGFR2/AKT/PLC-γ cascades following either cDNA transient transfection (B) or siRNA (C) treatment of DAB2IP in human HCC cells. Protein lysates were subjected to western blot analysis with specific antibodies. For each protein, densities were calculated by ImageQuaNT 5.1 software (GE Healthcare, Piscataway, NJ) and normalized to β-Actin (Chemicon International,Temecula, CA; dilution 1:20000) levels. Each bar respresents mean + SD. Multiple comparsion test (Kruskal-Wallis) $p < 0.05$ (A): *a, vs.* NL; *b, vs*. SL; *c vs*. HCCB; (B) *a* and *b* different from 24 and 48 h empty vector; (C) *a* and *b* different from 24 and 48 h scrambled.

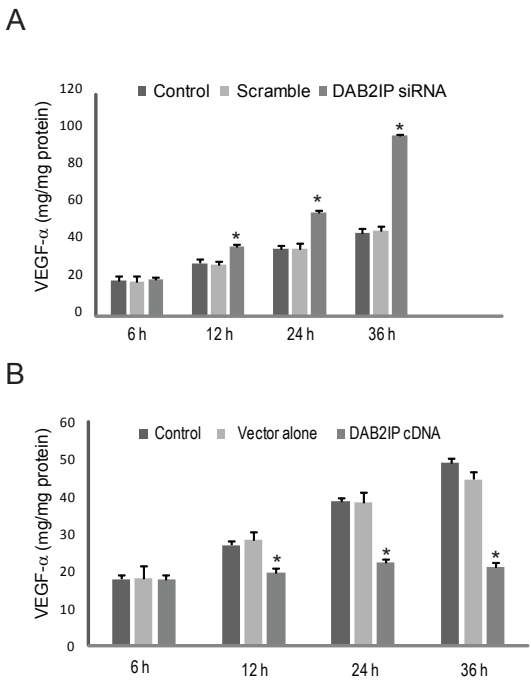

Supplementary Figure 7. Effect of DAB2IP modulation on VEGF-α secretion in human HCC cell lines. (A) Effect of DAB2IP silencing via siRNA on VEGF-α secretion in the medium of HuH6 cells. (B) Effect of DAB2IP overexpression via transient transfection on VEGF-α secretion in the medium of SNU449 cells. Experiments were repeated at least 3 times in triplicate, and results shown in (A) were reproduced in Hep3B cells (not shown). Each bar represents mean ± SD. Kruskal-Wallis test $p < 0.05$: (A) *, different from scrambled; (B) *, different from vector alone.

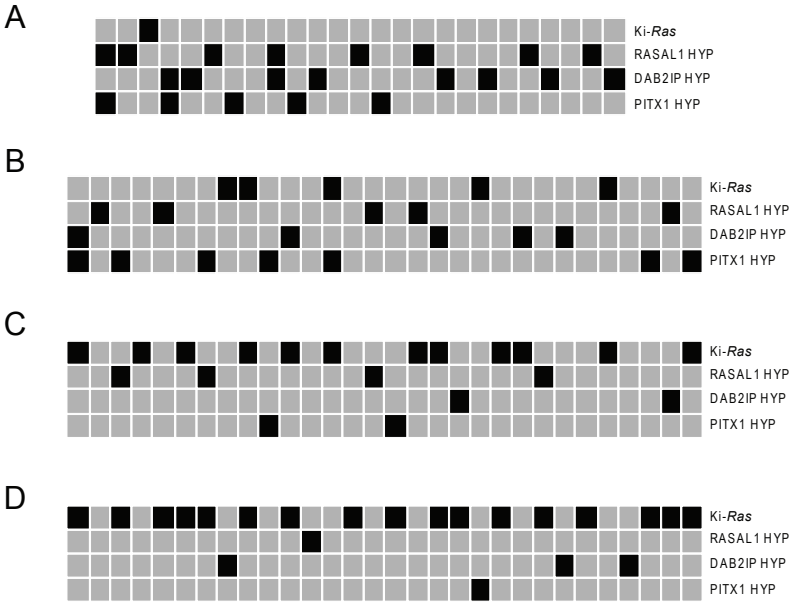

Supplementary Figure 8. Frequency of Ki-Ras mutations and promoter hypermethylation (HYP) of RASAL1, DAB2IP, PITX1 genes in human breast (A), lung (B), colon (C), and pancreatic (D) tumors. Presence of Ki-Ras mutations and/or promoter hypermethylation or absence of the same alterations is indicated by black and grey squares, respectively.

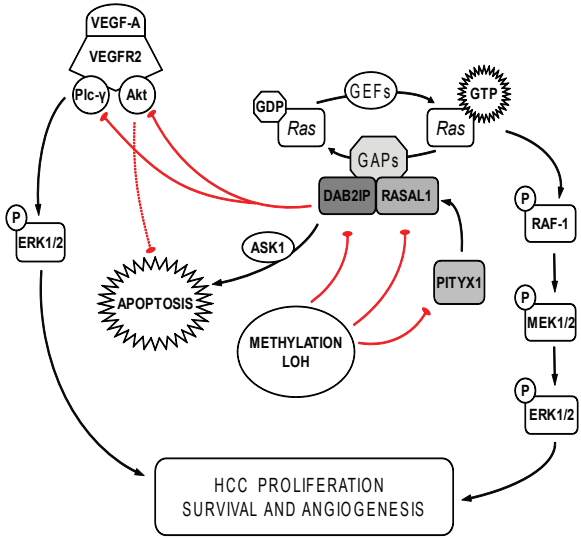

Supplementary Figure 9. Overview of signalling pathways aberrantly regulated following inactivation of RASAL1 and DAB2IP Ras GAPs in human HCC. In normal cells, RASAL1 and DAB2IP negatively regulate Ras activity by triggering conversion of GTP into GDP. In human HCC, inactivation of RASAL1, DAB2IP, and PITX1 (a RASAL1 inducer) by promoter hypermethylation and/or loss of heterozygosity (LOH) triggers unconstrained activity of the Ras pathway and promotes uncontrolled cell growth. Furthermore, loss of DAB2IP results in aberrant activation of the VEGFR2/AKT/PLC-γ cascade and in suppression of ASK1-dependent apoptosis.